

EPR spectrum via entangled states for an exchange-coupled dimer of single-molecule magnets

Xu Chang-Tan^{1,2,a} and J.-Q. Liang¹

¹ Institute of Theoretical Physics, Shanxi University, Taiyuan 030006, China

² Department of Physics, Linyi Normal University, Shandong Linyi 276005, China

and

Department of Physics, Qufu Normal University, Shandong Qufu 273165, China

Received 21 October 2004

Published online 30 May 2005 – © EDP Sciences, Società Italiana di Fisica, Springer-Verlag 2005

Abstract. Multi-high-frequency electron paramagnetic resonance(EPR) spectrum for a supermolecular dimer $[\text{Mn}_4]_2$ of single-molecule magnets recently reported [S. Hill, R.S. Edwards, N. Aliaga-Alcalde and G. Christou (HEAC), Science **302**, 1015 (2003)] is studied in terms of the perturbation method in which the high-order corrections to the level splittings of degenerate states are included. It is shown that the corresponding eigenvectors are composed of entangled states of two molecules. The EPR-peak positions are calculated in terms of the eigenstates at various frequencies. From the best fit of theoretical level splittings with the measured values we obtain the anisotropy constant and exchange coupling which are in agreement with the corresponding values of experimental observation. Our study confirms the prediction of HEAC that the two Mn_4 units within the dimer are coupled quantum mechanically by the antiferromagnetic exchange interaction and the supermolecular dimer behaviors in analogy with artificially fabricated quantum dots.

PACS. 75.45.+j Macroscopic quantum phenomena in magnetic systems – 75.50.Xx Molecular magnets – 75.50.Tt Fine-particle systems; nanocrystalline materials

1 Introduction

Single-molecule magnets(SMM), which may be the smallest nanomagnets exhibiting magnetization hysteresis-loop (a classical property of macroscopic magnets), straddle the interface between the characteristics of classical and quantum worlds. The quantum tunneling of magnetization and quantum phase interference known as macroscopic quantum effects have become an attractive research field in recent years. The quantum effects in these magnetic particles and clusters of nanometer size, such as $\text{Mn}_{12}(S = 10)$, $\text{Fe}_8(S = 10)$ and $\text{Mn}_4(S = \frac{9}{2})$ molecules, have been well studied [1–17] both experimentally and theoretically. Several proposals of possible quantum computing schemes are also suggested using molecular magnets [18–20]. The high-frequency single crystal electron paramagnetic resonance(EPR) is a powerful tool for the experimental study of various properties of single-molecule magnets [21–24]. Wernsdorfer et al. [25] recently pointed out that the supermolecular dimer $[\text{Mn}_4]_2$ consisting of two molecule magnets Mn_4 with antiferromagnetic exchange-coupling exhibits a quite different quantum behavior from two individual Mn_4 molecules without

coupling [25–28]. It is therefore of great importance to understand the effect of the exchange interaction which leads to energy level splitting [27,31] and has been studied with the high-order perturbation method [29]. The step-like magnetization hysteresis-loop in a supermolecular dimer have been demonstrated in terms of the numerical solution of the time-dependent Schrödinger equation [30]. Recently the multi-high-frequency EPR was used to probe the magnetic excitations of the supermolecular dimer $[\text{Mn}_4]_2$ by Hill et al. [31]. The measured spectra well interpret both the quantum transitions involving coherent superposition states of the two molecules and the phase decoherence rate, which provide a compelling evidence that the molecules are coupled quantum mechanically by the antiferromagnetic exchange interaction. In this paper, we restudy the EPR transitions in the supermolecular dimer $[\text{Mn}_4]_2$ employing the high-order perturbation method [29,32] and obtain the high-order corrections of level splitting. In terms of the corresponding eigenvectors accurate values of the anisotropy constant D and the antiferromagnetic exchange-coupling J are determined by the best fit between the theoretical and measured level-splitting. The EPR- peak positions are also calculated as a function of frequencies.

^a e-mail: xuchangtan@yahoo.com.cn

We in the following section first construct the explicit eigenvectors which are seen to be composed of entangled states. It is then shown that the ground states of the dimer are nearly (with probability 0.99883) the maximum entangled states, or Bell states which are useful in the quantum computing. The main goal of this work is to display all eigenvalues and the entanglements of the corresponding eigenstates in the dimer system. Our theoretical studies shine more light on the prediction of Hill et al. [31] that the supermolecular dimer with proper chemical design may be used as practical quantum devices for quantum computing.

2 Level splitting and eigenvectors

Neglecting off-diagonal crystal field terms and intermolecular interactions, the effective spin Hamiltonian with a magnetic field applied parallel to the easy axis of an isolate SMM has the form [31] $\hat{H}_i = -D_0 \hat{S}_{iz}^2 - B_4^0 \hat{O}_4^0 + g_z \mu_B B_z \hat{S}_{iz}$, where \hat{S}_{iz} is the z -axis spin projection operator, and the index $i (= 1, 2)$ is used to label the two Mn_4 molecules in the dimer; $D_0 > 0$ denotes the uniaxial anisotropy constant; $B_4^0 \hat{O}_4^0$ characterizes the fourth order uniaxial anisotropy where $\hat{O}_4^0 = 35 \hat{S}_z^4 - [30S(S+1) - 25] \hat{S}_z^2 - 6S(S+1) + 3S^2(S+1)^2$; g is the electronic g -factor; and μ_B is the Bohr magneton. The Hamiltonian \hat{H}_i may be written in the following form apart from a trivial constant

$$\hat{H}_i = -D \hat{S}_{iz}^2 - B \hat{S}_{iz}^4 + g_z \mu_B B_z \hat{S}_{iz}, \quad (1)$$

where $D = D_0 - 30S(S+1) - 25$, $B = 35B_4^0$.

For the supermolecular dimer with antiferromagnetic coupling the Hamiltonian is seen to be

$$\hat{H} = [\hat{H}_1 + \hat{H}_2 + J_z \hat{S}_{1z} \hat{S}_{2z}] + \frac{1}{2} J_{xy} (\hat{S}_{1+} \hat{S}_{2-} + \hat{S}_{1-} \hat{S}_{2+}), \quad (2)$$

where $\hat{S}_{\pm} = \hat{S}_x \pm i \hat{S}_y$ with J_z and J_{xy} denoting the strengths of exchange coupling. In the following we consider only the isotropic case that $J_z = J_{xy} = J > 0$ which has been verified experimentally [27]. We furthermore assume that the exchange coupling J is much less than the anisotropy constant D . Then, \hat{H} is rewritten as the perturbation form

$$\hat{H} = \hat{H}_0 + \hat{V}, \quad (3)$$

$$\begin{aligned} \hat{H}_0 &= -D (\hat{S}_{1z}^2 + \hat{S}_{2z}^2) - B (\hat{S}_{1z}^4 + \hat{S}_{2z}^4) + J \hat{S}_{1z} \hat{S}_{2z} \\ &\quad + g_z \mu_B H_z (\hat{S}_{1z} + \hat{S}_{2z}), \end{aligned} \quad (4)$$

$$\hat{V} = \frac{1}{2} J (\hat{S}_{1+} \hat{S}_{2-} + \hat{S}_{1-} \hat{S}_{2+}), \quad (5)$$

where \hat{H}_0 is the zeroth-order Hamiltonian. The zeroth-order eigenvectors of the dimer are direct products of the single-molecule eigenvectors such that $|S_1, S_2, M_1, M_2\rangle$ or abbreviated as $|M_1, M_2\rangle$, where M_1 and M_2 represent the

quantum numbers of spin operators \hat{S}_{1z} and \hat{S}_{2z} respectively. The dimer has $(2S_1+1)(2S_2+1)$ energy levels which are labeled by the spin quantum numbers M_1 and M_2 and given by

$$\begin{aligned} E_0 &= -D (M_1^2 + M_2^2) - B (M_1^4 + M_2^4) + JM_1 M_2 \\ &\quad + g_z \mu_B H_z (M_1 + M_2). \end{aligned} \quad (6)$$

It is seen obviously that the eigenstates $|M_1, M_2\rangle$ and $|M_2, M_1\rangle$ are degenerate since $E_0(M_1, M_2) = E_0(M_2, M_1)$. The two Mn_4 molecules in the $[Mn_4]_2$ dimer are coupled by a weak exchange interaction via both the six C-H \cdots Cl hydrogen bonds. Thus, we can treat \hat{V} perturbationally.. The level splitting of the pair of degenerate eigenstates $|M_1, M_2\rangle$ and $|M_2, M_1\rangle$ with $M_2 > M_1$ appears only in the chain of matrix elements connecting the states $|M_1+k, M_2-k\rangle$ and $|M_1+k+1, M_2-k-1\rangle$, where $k = 1, 2, \dots, M_2 - M_1 - 1$. Then, the level splitting becomes [29,32]

$$\begin{aligned} \Delta E_{M_1 M_2, M_2 M_1} &= 2 \hat{V}_{M_1 M_2, (M_1+1)(M_2-1)} \\ &\quad \times \frac{1}{E_{(M_1+1)(M_2-1)} - E_{M_1 M_2}} \hat{V}_{(M_1+1)(M_2-1), (M_1+2)(M_2-2)} \\ &\quad \times \frac{1}{E_{(M_1+2)(M_2-2)} - E_{M_1 M_2}} \dots \hat{V}_{(M_2-1)(M_1+1), M_2 M_1}, \end{aligned} \quad (7)$$

where

$$\begin{aligned} \hat{V}_{M_1 M_2, (M_1+1)(M_2-1)} &= \langle M_1, M_2 | \frac{1}{2} J (\hat{S}_{1+} \hat{S}_{2-} + \hat{S}_{1-} \hat{S}_{2+}) \\ &\quad \times |M_1+1, M_2-1\rangle = \frac{J}{2} h_{(M_1+1)(M_2-1)}, \end{aligned} \quad (8)$$

and

$$\begin{aligned} h_{(M_1+1)(M_2-1)} &= \left[(S_1 + M_1 + 1)(S_1 - M_1) \right. \\ &\quad \times (S_2 - M_2 + 1)(S_2 + M_2) \left. \right]^{\frac{1}{2}}. \end{aligned} \quad (9)$$

Since $S_1 = S_2 = S$ for the dimer case, we obtain the level splitting as

$$\begin{aligned} \Delta E &= \left\{ \prod_k \left[2D' - 4Bk(M_2 - M_1 - k) \right] \right\}^{-1} \\ &\quad \times \frac{J^{M_2 - M_1}}{[(M_1 - M_2 - 1)!]^2} \frac{(S + M_2)!(S - M_1)!}{(S - M_2)!(S + M_1)!}, \end{aligned} \quad (10)$$

where

$$D' = 2D + J + 4B(M_1 + M_2)^2 - 4BM_1 M_2. \quad (11)$$

Disregarding the fourth- power of anisotropy term in equation (4) i.e. $B = 0$, the formula of level splitting can be simplified as

$$\begin{aligned} \Delta E &= (4D + 2J) \left(\frac{J}{4D + 2J} \right)^{M_2 - M_1} \\ &\quad \times \frac{(S + M_2)!(S - M_1)!}{(S - M_2)!(S + M_1)!} \left[\frac{1}{(M_2 - M_1 - 1)!} \right]^2. \end{aligned} \quad (12)$$

The state of the zeroth-order perturbation is obviously the superposition of the states $|M_1, M_2\rangle$ and $|M_2, M_1\rangle$ such that

$$|\psi^{(0)}\rangle = a_{M_1 M_2}^{(0)} |M_1, M_2\rangle + a_{M_2 M_1}^{(0)} |M_2, M_1\rangle. \quad (13)$$

The first-order state is then obtained as

$$|\psi^{(1)}\rangle = \sum_{k_1, k_2} a_{k_1 k_2}^{(1)} |k_1, k_2\rangle, \quad (14)$$

where

$$a_{k_1 k_2}^{(1)} = \frac{a_{M_1 M_2}^{(0)} \hat{V}_{k_1 k_2, M_1 M_2} + a_{M_2 M_1}^{(0)} \hat{V}_{k_1 k_2, M_2 M_1}}{E_{M_2 M_1} - E_{k_1 k_2}}, \quad (15)$$

and $a_{M_1 M_2}^{(1)} = a_{M_2 M_1}^{(1)} = 0$. The n th order state is

$$|\psi^{(n)}\rangle = \sum_{k_1, k_2} a_{k_1 k_2}^{(n)} |k_1, k_2\rangle, \quad (16)$$

where

$$a_{k_1 k_2}^{(n)} = \sum_{k'_1, k'_2} \frac{\hat{V}_{k_1 k_2, k'_1 k'_2}}{E_{M_2 M_1} - E_{k_1 k_2}} a_{k'_1 k'_2}^{(n-1)}, \quad (17)$$

and $(k_1, k_2) \neq (k'_1, k'_2) \neq (M_1, M_2) \neq (M_2, M_1)$, $a_{M_1 M_2}^{(m)} = a_{M_2 M_1}^{(m)} = 0$ ($m = 1, 2, \dots, n$). For $n = M_2 - k_1 = k_2 - M_1 \geq 1$, we have

$$\begin{aligned} a_{k_1 k_2}^{(n)} &= \frac{\hat{V}_{k_1 k_2, (k_1+1)(k_2-1)}}{E_{M_2 M_1} - E_{k_1 k_2}} \frac{\hat{V}_{(k_1+1)(k_2-1), (k_1+2)(k_2-2)}}{E_{M_2 M_1} - E_{k_1+1, k_2-1}} \\ &\times \frac{\hat{V}_{(k_1+2)(k_2-2), (k_1+3)(k_2-3)}}{E_{M_2 M_1} - E_{k_1+2, k_2-2}} \dots \frac{\hat{V}_{(M_2-1)(M_1+1), M_2 M_1}}{E_{M_2 M_1} - E_{M_2-1, M_1+1}}, \end{aligned} \quad (18)$$

and

$$\begin{aligned} \hat{V}_{(k_1+l-1)(k_2-l+1), (k_1+l)(k_2-l)} &= \frac{J}{2} \langle k_1 + l - 1, k_2 - l + 1 | \\ &\quad \times \hat{S}_{1-} \hat{S}_{2+} |k_1 + l, k_2 - l\rangle \\ &= \frac{J}{2} \left[(S - k_2 + l) (S + k_2 + 1 - l) \right. \\ &\quad \left. \times (S + k_1 + l) (S - k_1 + 1 - l) \right]^{\frac{1}{2}}, \end{aligned} \quad (19)$$

where $l = 1, 2, \dots, n$. We finally obtain the coefficients $a_{k_1 k_2}^{(n)}$ of the n th order state

$$\begin{aligned} a_{k_1 k_2}^{(n)} &= J^n \left\{ \prod_{l=0}^{n-1} [M_{12} + l (k_1 - k_2 + l)] \right. \\ &\quad \left. \times \left[2D'' + 4Bl (k_1 - k_2 + l) \right] \right\}^{-1} \\ &\times \left[\frac{(S + M_2)! (S - M_1)! (S - k_1)! (S + k_2)!}{(S - M_2)! (S + M_1)! (S + k_1)! (S - k_2)!} \right]^{\frac{1}{2}}, \end{aligned} \quad (20)$$

where $M_{12} = M_1 M_2 - k_1 k_2$, $D'' = 2D + J + 4B(M_1 + M_2)^2 - 2B(M_1 M_2 + k_1 k_2)$. For the case $n' = k'_1 - M_1 = M_2 - k'_2 \geq 1$, we have

$$\begin{aligned} a_{k'_1 k'_2}^{(n')} &= J^{n'} \left\{ \prod_{l=0}^{n'-1} \left[M'_{12} + l (k'_2 - k'_1 + l) \right] \right. \\ &\quad \left. \times \left[2D''' + 4Bl (k'_2 - k'_1 + l) \right] \right\}^{-1} \\ &\times \left[\frac{(S + M_2)! (S - M_1)! (S - k'_2)! (S + k'_1)!}{(S - M_2)! (S + M_1)! (S + k'_2)! (S - k'_1)!} \right]^{\frac{1}{2}}, \end{aligned} \quad (21)$$

where $M'_{12} = M_1 M_2 - k'_1 k'_2$, $D''' = 2D + J + 4B(M_1 + M_2)^2 - 2B(M_1 M_2 + k'_1 k'_2)$.

The zeroth-order perturbation wave functions for the non-degenerate states $|M_1, M_2\rangle$ with $M_1 = M_2 = M$ are seen to be $|\psi^{(0)}\rangle = 2|M, M\rangle$. The matrix elements of operator \hat{V} in equation (18) appear only in the chain connecting the states $|k_1 + l, k_2 - l\rangle$ and $|k_1 + l + 1, k_2 - l - 1\rangle$. We can obtain the results by non-degenerate perturbation theory as follows. When $a_{k_1 k_2}^{(n)} \neq 0$, $a_{k_1 k_2}^{(1)} = a_{k_1 k_2}^{(2)} = \dots = a_{k_1 k_2}^{(n-1)} = 0$, as a consequence equations (16, 17, 20) and (21) become the same as for the case of non-degenerate states.

Making use of equations (13, 16, 20) and (21), we can obtain all eigenvectors for the quantum number range from $M = M_1 + M_2 = -9$ to 0 , while the eigenvectors for the quantum number range from $M = 1$ to 9 can be obtained simply by the replacements: $M_1 \rightarrow -M_1, M_2 \rightarrow -M_2$ in the former case. The eigenstates are listed in Appendix A (where $|M_1, M_2\rangle_S$ and $|M_1, M_2\rangle_A$ denote the symmetric and antisymmetric states respectively) with parameter values $D = 0.72$ K, $B = 1.8 \times 10^{-3}$ K, $J = 0.10$ K which give rise to the best fit between theoretical and measured level splitting. The parameters D and B determined here with the best fit are in agreement with the values obtained by Hill et al. [31]. When $M_1 \neq M_2$, the normalized symmetric $|M_1, M_2\rangle_S$ and the antisymmetric $|M_1, M_2\rangle_A$ states are actually maximum entangled states with the entanglement degree of von Neumann entropy that $E(\rho) = 1$, where

$$E(\rho) = \text{Tr} \rho \log_2 \rho,$$

and ρ is the reduced density matrix [33]. When $M_1 = M_2$, the states are disentangled. Thus, the eigenvectors are, in general, composed of maximum entangled states with definite probabilities. For example, $|\psi_1\rangle_S$ is the disentangled state and $|\psi_2\rangle_S, |\psi_2\rangle_A, |\psi_3\rangle_A$ are maximum entangled states with $E(\rho) = 1$. The state $|\psi_5\rangle_A$ is composed of maximum entangled states $\frac{1}{\sqrt{2}} |-\frac{9}{2}, -\frac{3}{2}\rangle_A$ and $\frac{1}{\sqrt{2}} |-\frac{7}{2}, -\frac{5}{2}\rangle_A$ with probabilities 0.9445 and 0.0555 respectively. Moreover, the probability of the maximum entangled states $\frac{1}{\sqrt{2}} |-\frac{9}{2}, \frac{9}{2}\rangle_{S,A}$ which emerge in the

Table 1. The resonant field transitions. Theoretical values are obtained by the high-order level splitting formula and eigenvectors with parameter values $D = 0.72$ K, $B = 1.8 \times 10^{-3}$ K and $J = 0.10$ K.

sign	transition	resonance field B_z [T]		sign	transition	resonance field B_z [T]	
		calc	exp ²⁷			calc	exp ²⁷
x	$ \psi_{26}\rangle_{S4} \rightarrow \psi_{31}\rangle_{S4}$	0.234	0.21 ± 0.05	a	$ \psi_1\rangle_S \rightarrow \psi_2\rangle_S$	0.546	0.53 ± 0.05
b	$ \psi_2\rangle_S \rightarrow \psi_4\rangle_S$	0.931	1.00 ± 0.05	c	$ \psi_2\rangle_A \rightarrow \psi_3\rangle_A$	1.817	1.80 ± 0.05
l	$ \psi_2\rangle_S \rightarrow \psi_3\rangle_S$	2.783	2.75 ± 0.05	d	$ \psi_3\rangle_A \rightarrow \psi_6\rangle_A$	1.327	1.40 ± 0.05
j	$ \psi_3\rangle_S \rightarrow \psi_6\rangle_S$	-0.159	—	e	$ \psi_4\rangle_S \rightarrow \psi_6\rangle_S$	1.693	1.70 ± 0.05
g	$ \psi_3\rangle_A \rightarrow \psi_5\rangle_A$	3.450	3.45 ± 0.05	f	$ \psi_3\rangle_S \rightarrow \psi_5\rangle_S$	3.107	3.20 ± 0.05
m	$ \psi_4\rangle_S \rightarrow \psi_5\rangle_S$	4.959	4.85 ± 0.05	h	$ \psi_5\rangle_A \rightarrow \psi_7\rangle_A$	4.391	4.5 ± 0.05
h	$ \psi_5\rangle_S \rightarrow \psi_7\rangle_S$	4.434	4.5 ± 0.05	k	$ \psi_6\rangle_A \rightarrow \psi_7\rangle_A$	6.513	—
r	$ \psi_6\rangle_S \rightarrow \psi_7\rangle_S$	7.700	—	s	$ \psi_5\rangle_A \rightarrow \psi_8\rangle_A$	0.457	—
s'	$ \psi_5\rangle_S \rightarrow \psi_8\rangle_S$	-0.241	—	t	$ \psi_6\rangle_A \rightarrow \psi_8\rangle_A$	2.579	—
o	$ \psi_6\rangle_S \rightarrow \psi_8\rangle_S$	3.025	—	I	$ \psi_5\rangle_S \rightarrow \psi_9\rangle_S$	-1.16	—
n	$ \psi_6\rangle_S \rightarrow \psi_9\rangle_S$	2.106	2.20 ± 0.05	i	$ \psi_7\rangle_A \rightarrow \psi_{10}\rangle_A$	5.437	5.50 ± 0.05
i	$ \psi_7\rangle_S \rightarrow \psi_{10}\rangle_S$	5.441	5.50 ± 0.05	3	$ \psi_8\rangle_A \rightarrow \psi_{10}\rangle_A$	9.371	—
4	$ \psi_8\rangle_S \rightarrow \psi_{10}\rangle_S$	10.116	—	2	$ \psi_9\rangle_S \rightarrow \psi_{10}\rangle_S$	11.035	—
	$ \psi_7\rangle_S \rightarrow \psi_{11}\rangle_S$	0.440	—		$ \psi_7\rangle_A \rightarrow \psi_{11}\rangle_A$	0.576	—
	$ \psi_8\rangle_A \rightarrow \psi_{11}\rangle_A$	4.510	—		$ \psi_8\rangle_S \rightarrow \psi_{11}\rangle_S$	5.114	—
	$ \psi_9\rangle_S \rightarrow \psi_{11}\rangle_S$	6.034	—		$ \psi_7\rangle_A \rightarrow \psi_{12}\rangle_A$	-1.147	—
	$ \psi_7\rangle_S \rightarrow \psi_{12}\rangle_S$	-2.705	—		$ \psi_8\rangle_A \rightarrow \psi_{12}\rangle_A$	2.788	—
	$ \psi_8\rangle_S \rightarrow \psi_{12}\rangle_S$	1.970	—		$ \psi_9\rangle_S \rightarrow \psi_{12}\rangle_S$	2.889	—
u	$ \psi_{10}\rangle_{S4} \rightarrow \psi_{13}\rangle_{S4}$	6.642	—		$ \psi_{11}\rangle_A \rightarrow \psi_{13}\rangle_A$	11.504	—
	$ \psi_{11}\rangle_S \rightarrow \psi_{13}\rangle_S$	11.644	—		$ \psi_{12}\rangle_A \rightarrow \psi_{13}\rangle_A$	13.226	—
	$ \psi_{12}\rangle_S \rightarrow \psi_{13}\rangle_S$	14.789	—		$ \psi_{10}\rangle_A \rightarrow \psi_{14}\rangle_A$	0.608	—

states $|\psi_{26}\rangle_{S,A}$ is 0.99883. It is also seen that the ground states $|\psi_{26}\rangle_S$ and $|\psi_{26}\rangle_A$ are very close to the maximum entangled states in a small range of magnetic field values.

3 EPR transition

In the EPR experiment, it has been seen that the exchange-coupling induced single-spin transitions i.e. the transitions from (M_1, M_2) to $(M_1 + 1, M_2)$ or from (M_1, M_2) to $(M_1, M_2 + 1)$ can occur, however, the single-spin transitions should also depend on the states of the other spin within the dimer because of the exchange coupling. This dependence has displayed its importance in the resonant macroscopic quantum tunneling too. Most importantly the multi-high-frequency electron paramagnetic resonance spectra of the dimer obtained by Wernsdorfer et al. [27] and Hill et al. [31] show a compelling evidence that the two molecules Mn_4 are coupled quantum mechanically by the antiferromagnetic exchange-coupling

which leads to the energy level splitting. In terms of equation (6) and equation (10), we can calculate the energy level splitting caused by the perturbation part of the Hamiltonian \hat{V} . Thus, when the frequency ν is fixed to the value 145 GHz and the magnetic field B_z varies quasi-statically to reach a resonance point, the EPR transition matrix elements with the selection rule $\Delta M = \pm 1$ can be accurately calculated using the level splitting formula equation (10) with the help of the corresponding eigenvectors shown in Appendix A. The magnetic dipole perturbation allows transitions only between states of the same symmetry. The positions of principal and other possible EPR peaks are given in Table 1 (resonance transitions between higher energy levels are not listed), and displayed schematically in Figure 1. From Table 1, we can find that principal resonance peaks labeled by (x), (a) to (i) are in agreement with the result of Hill et al. [31] (see Fig. 2 and Fig. 3 in Ref. [31]). From the Figure 3 of reference [31] we can see that the resonance peaks labeled by (l), (m), (n), (p) and (q) with magnetic field

Table 1. Continued.

	$ \psi_{10}\rangle_S \rightarrow \psi_{14}\rangle_S$	0.596	—	$ \psi_{11}\rangle_A \rightarrow \psi_{14}\rangle_A$	5.470	—
	$ \psi_{11}\rangle_S \rightarrow \psi_{14}\rangle_S$	5.598	—	$ \psi_{12}\rangle_A \rightarrow \psi_{14}\rangle_A$	7.192	—
	$ \psi_{12}\rangle_S \rightarrow \psi_{14}\rangle_S$	8.742	—	$ \psi_{10}\rangle_A \rightarrow \psi_{15}\rangle_A$	-3.226	—
	$ \psi_{10}\rangle_S \rightarrow \psi_{15}\rangle_S$	-4.404	—	$ \psi_{11}\rangle_A \rightarrow \psi_{15}\rangle_A$	1.635	—
	$ \psi_{11}\rangle_S \rightarrow \psi_{15}\rangle_S$	0.598	—	$ \psi_{12}\rangle_A \rightarrow \psi_{15}\rangle_A$	3.358	3.55 ± 0.05
<i>q</i>	$ \psi_{12}\rangle_S \rightarrow \psi_{15}\rangle_S$	3.742	3.80 ± 0.05	$ \psi_{10}\rangle_S \rightarrow \psi_{16}\rangle_S$	-4.285	—
	$ \psi_{11}\rangle_S \rightarrow \psi_{16}\rangle_S$	0.717	—	$ \psi_{12}\rangle_S \rightarrow \psi_{16}\rangle_S$	1.319	—
<i>v</i>	$ \psi_{13}\rangle_{S4} \rightarrow \psi_{17}\rangle_{S4}$	7.654	—	$ \psi_{14}\rangle_A \rightarrow \psi_{17}\rangle_A$	13.688	—
	$ \psi_{14}\rangle_S \rightarrow \psi_{17}\rangle_S$	13.70	—	$ \psi_{15}\rangle_A \rightarrow \psi_{17}\rangle_A$	17.523	—
	$ \psi_{15}\rangle_S \rightarrow \psi_{17}\rangle_S$	18.70	—	$ \psi_{16}\rangle_S \rightarrow \psi_{17}\rangle_S$	18.581	—
	$ \psi_{13}\rangle_A \rightarrow \psi_{18}\rangle_A$	0.386	—	$ \psi_{13}\rangle_S \rightarrow \psi_{18}\rangle_S$	0.385	—
	$ \psi_{14}\rangle_A \rightarrow \psi_{18}\rangle_A$	6.419	—	$ \psi_{14}\rangle_S \rightarrow \psi_{18}\rangle_S$	6.431	—
	$ \psi_{15}\rangle_A \rightarrow \psi_{18}\rangle_A$	10.254	—	$ \psi_{15}\rangle_S \rightarrow \psi_{18}\rangle_S$	11.431	—
	$ \psi_{16}\rangle_S \rightarrow \psi_{18}\rangle_S$	11.312	—	<i>w</i> $ \psi_{17}\rangle_{S4} \rightarrow \psi_{21}\rangle_{S4}$	8.901	—
	$ \psi_{18}\rangle_{S4} \rightarrow \psi_{21}\rangle_{S4}$	16.170	—	$ \psi_{19}\rangle_A \rightarrow \psi_{21}\rangle_A$	20.79	—
	$ \psi_{19}\rangle_S \rightarrow \psi_{21}\rangle_S$	21.027	—	$ \psi_{20}\rangle_A \rightarrow \psi_{21}\rangle_A$	22.353	—
	$ \psi_{20}\rangle_S \rightarrow \psi_{21}\rangle_S$	24.14	—	$ \psi_{17}\rangle_{S4} \rightarrow \psi_{22}\rangle_{S4}$	0.415	—
	$ \psi_{18}\rangle_{S4} \rightarrow \psi_{22}\rangle_{S4}$	7.684	—	$ \psi_{19}\rangle_A \rightarrow \psi_{22}\rangle_A$	12.304	—
	$ \psi_{19}\rangle_S \rightarrow \psi_{22}\rangle_S$	12.542	—	$ \psi_{20}\rangle_A \rightarrow \psi_{22}\rangle_A$	13.867	—
	$ \psi_{20}\rangle_S \rightarrow \psi_{22}\rangle_S$	15.653	—	$ \psi_{17}\rangle_A \rightarrow \psi_{23}\rangle_A$	-5.451	—
	$ \psi_{17}\rangle_S \rightarrow \psi_{23}\rangle_S$	-5.472	—	$ \psi_{18}\rangle_A \rightarrow \psi_{23}\rangle_A$	1.814	—
	$ \psi_{18}\rangle_S \rightarrow \psi_{23}\rangle_S$	1.798	—	$ \psi_{19}\rangle_A \rightarrow \psi_{23}\rangle_A$	6.438	—
	$ \psi_{19}\rangle_S \rightarrow \psi_{23}\rangle_S$	6.655	—	$ \psi_{20}\rangle_A \rightarrow \psi_{23}\rangle_A$	8.001	—
	$ \psi_{20}\rangle_S \rightarrow \psi_{23}\rangle_S$	9.766	—	<i>y</i> $ \psi_{21}\rangle_{S4} \rightarrow \psi_{26}\rangle_{S4}$	10.125	—
	$ \psi_{22}\rangle_{S4} \rightarrow \psi_{26}\rangle_{S4}$	18.611	—	$ \psi_{21}\rangle_{S4} \rightarrow \psi_{27}\rangle_{S4}$	0.262	—
	$ \psi_{22}\rangle_{S4} \rightarrow \psi_{27}\rangle_{S4}$	8.748	—	$ \psi_{23}\rangle_A \rightarrow \psi_{27}\rangle_A$	14.615	—
	$ \psi_{23}\rangle_S \rightarrow \psi_{27}\rangle_S$	14.635	—	$ \psi_{21}\rangle_{S4} \rightarrow \psi_{28}\rangle_{S4}$	-6.91	—
	$ \psi_{22}\rangle_{S4} \rightarrow \psi_{28}\rangle_{S4}$	1.576	—	$ \psi_{23}\rangle_A \rightarrow \psi_{28}\rangle_A$	7.442	—
	$ \psi_{23}\rangle_S \rightarrow \psi_{28}\rangle_S$	7.463	—	$ \psi_{27}\rangle_{S4} \rightarrow \psi_{31}\rangle_{S4}$	10.10	—
	$ \psi_{28}\rangle_{S4} \rightarrow \psi_{31}\rangle_{S4}$	17.27	—	$ \psi_{26}\rangle_{S4} \rightarrow \psi_{32}\rangle_{S4}$	-8.251	—
	$ \psi_{27}\rangle_{S4} \rightarrow \psi_{32}\rangle_{S4}$	1.612	—	$ \psi_{28}\rangle_{S4} \rightarrow \psi_{32}\rangle_{S4}$	8.784	—
<i>z</i>	$ \psi_{31}\rangle_{S4} \rightarrow \psi_{33}\rangle_{S4}$	1.459	—	$ \psi_{32}\rangle_{S4} \rightarrow \psi_{33}\rangle_{S4}$	9.945	—
	$ \psi_{31}\rangle_{S4} \rightarrow \psi_{34}\rangle_{S4}$	-5.81	—	$ \psi_{32}\rangle_{S4} \rightarrow \psi_{34}\rangle_{S4}$	2.676	—
<i>A</i>	$ \psi_{33}\rangle_{S4} \rightarrow \psi_{35}\rangle_{S4}$	2.706	—	$ \psi_{34}\rangle_{S4} \rightarrow \psi_{35}\rangle_{S4}$	9.975	—
<i>B</i>	$ \psi_{35}\rangle_{S4} \rightarrow \psi_{36}\rangle_{S4}$	3.718	—			

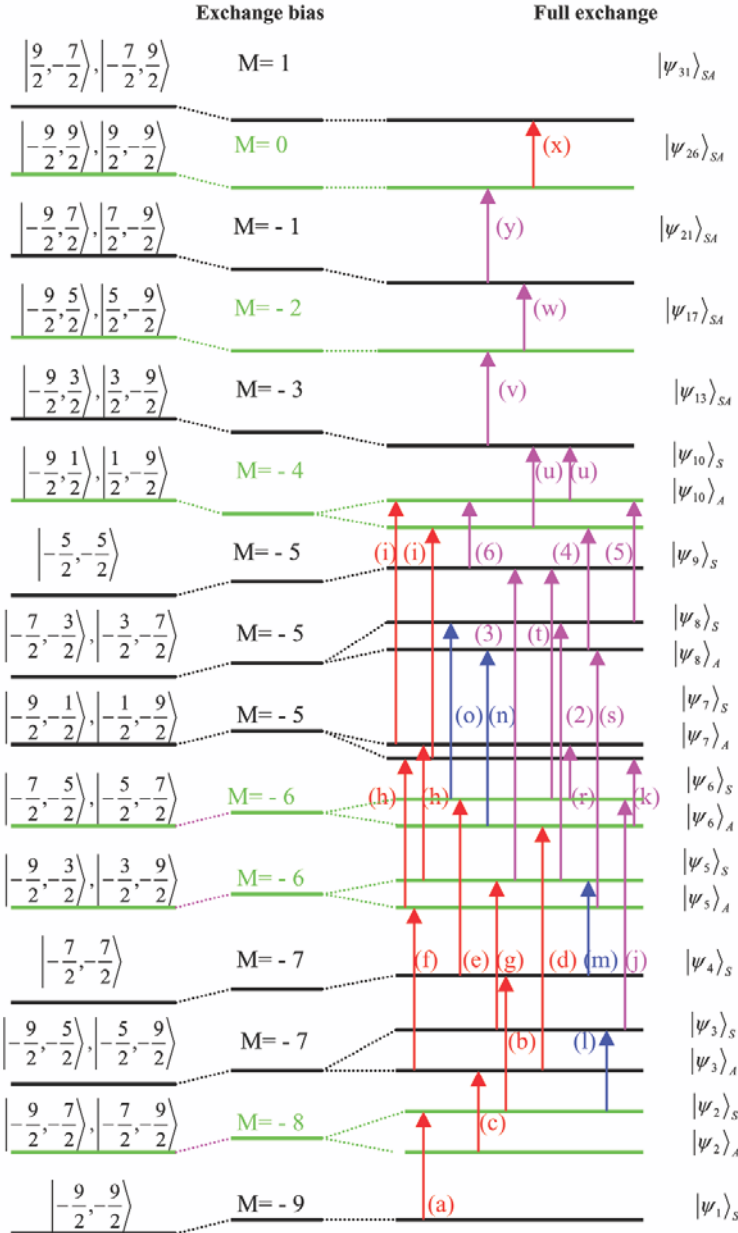


Fig. 1. Schematic display of lowest energy states ($M = -9$ to -4) and the part of lower energy states ($M = -3$ to 1). The zeroth-order energy levels and eigenvectors are shown on the left; energy shifts due to the exchange-interaction are shown in the center; and the results of the high-order perturbation calculation are displayed on the right. The red lines [x , (a) to (i)] denote the strongest EPR transitions; the blue lines denote the weaker EPR transitions; the magenta lines denote other possible EPR transitions.

values $B_z = 2.75 \pm 0.05, 4.85 \pm 0.05, 2.20 \pm 0.05, 3.55 \pm 0.05, 3.80 \pm 0.05$ respectively, are also in agreement with our result in Table 1. We expect that the possible EPR peaks calculated at the higher field region for $B_z \geq 6$ tesla can be verified by future EPR experiments. Moreover the relation between the field value B_z and frequency ν can be obtained from the resonance condition

$$\hbar\nu = E(M+1) - E(M) = \Delta E + g_z\mu_B B_z, \quad (22)$$

where the energy $E(M)$ can be accurately calculated from the level splitting formula equation (10) and the eigenvectors in Appendix A. The level splitting ΔE is shown in

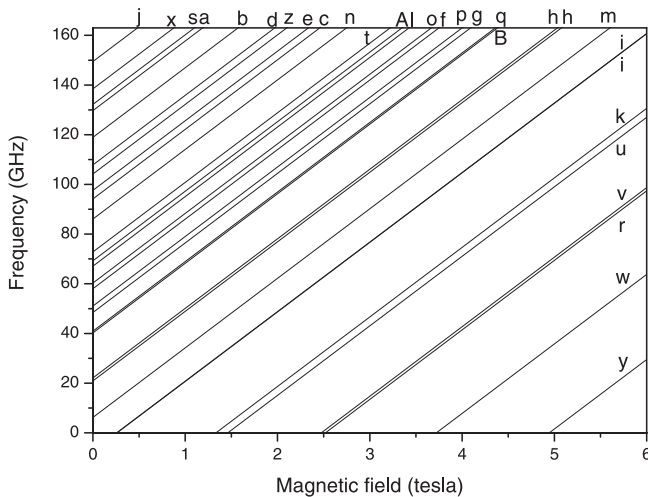
Table 2 for various EPR transitions. The calculated positions of EPR peaks depending on frequencies are shown in Figure 2.

4 Conclusion

The EPR spectra in the supermolecular dimer [Mn₄]₂ with the antiferromagnetic exchange-coupling between two molecule magnets are studied in terms of the high-order perturbation method which allows us to obtain the

Table 2. Level splitting ΔE in equation (22).

Sign	Eigenvectors	ΔE (K)	Sign	Eigenvectors	ΔE (K)
<i>x</i>	$ \psi_{26}\rangle_{SA} \rightarrow \psi_{31}\rangle_{SA}$	6.6466	<i>a</i>	$ \psi_1\rangle_S \rightarrow \psi_2\rangle_S$	6.228
<i>b</i>	$ \psi_2\rangle_S \rightarrow \psi_4\rangle_S$	5.7111	<i>c</i>	$ \psi_2\rangle_A \rightarrow \psi_5\rangle_A$	4.5198
<i>l</i>	$ \psi_2\rangle_S \rightarrow \psi_3\rangle_S$	3.2216	<i>d</i>	$ \psi_3\rangle_A \rightarrow \psi_6\rangle_A$	5.1780
<i>j</i>	$ \psi_3\rangle_S \rightarrow \psi_6\rangle_S$	7.1762	<i>e</i>	$ \psi_4\rangle_S \rightarrow \psi_6\rangle_S$	4.6867
<i>g</i>	$ \psi_3\rangle_A \rightarrow \psi_5\rangle_A$	2.3256	<i>f</i>	$ \psi_3\rangle_S \rightarrow \psi_5\rangle_S$	2.786
<i>m</i>	$ \psi_4\rangle_S \rightarrow \psi_5\rangle_S$	0.2965	<i>h</i>	$ \psi_5\rangle_A \rightarrow \psi_7\rangle_A$	1.0604
<i>h</i>	$ \psi_5\rangle_S \rightarrow \psi_7\rangle_S$	1.0034	<i>k</i>	$ \psi_6\rangle_A \rightarrow \psi_7\rangle_A$	-1.7920
<i>r</i>	$ \psi_6\rangle_S \rightarrow \psi_7\rangle_S$	-3.3868	<i>s</i>	$ \psi_5\rangle_A \rightarrow \psi_8\rangle_A$	6.3478
<i>t</i>	$ \psi_6\rangle_A \rightarrow \psi_8\rangle_A$	3.4954	<i>o</i>	$ \psi_6\rangle_S \rightarrow \psi_8\rangle_S$	2.8962
<i>n</i>	$ \psi_6\rangle_S \rightarrow \psi_9\rangle_S$	4.1316	<i>i</i>	$ \psi_7\rangle_A \rightarrow \psi_{10}\rangle_A$	-0.3458
<i>i</i>	$ \psi_7\rangle_S \rightarrow \psi_{10}\rangle_S$	-0.3510	<i>u</i>	$ \psi_{10}\rangle_{SA} \rightarrow \psi_{13}\rangle_{SA}$	-1.9650
<i>p</i>	$ \psi_{12}\rangle_A \rightarrow \psi_{15}\rangle_A$	2.4495	<i>q</i>	$ \psi_{12}\rangle_S \rightarrow \psi_{15}\rangle_S$	1.9322
<i>v</i>	$ \psi_{13}\rangle_{SA} \rightarrow \psi_{17}\rangle_{SA}$	-3.3252	<i>w</i>	$ \psi_{17}\rangle_{SA} \rightarrow \psi_{21}\rangle_{SA}$	-5.0012
<i>y</i>	$ \psi_{21}\rangle_{SA} \rightarrow \psi_{26}\rangle_{SA}$	-6.6466	<i>z</i>	$ \psi_{31}\rangle_{SA} \rightarrow \psi_{33}\rangle_{SA}$	5.0012
<i>A</i>	$ \psi_{33}\rangle_{SA} \rightarrow \psi_{35}\rangle_{SA}$	3.3252	<i>B</i>	$ \psi_{35}\rangle_{SA} \rightarrow \psi_{36}\rangle_{SA}$	1.9650

**Fig. 2.** EPR- peak positions (solid lines) obtained from equation (23) with different frequencies.

level splitting of the degenerate pairing states and the corresponding eigenvectors. It is shown that the eigenvectors are composed of maximum entangled states with definite probabilities. This observation shines more light on the potential application of molecular magnets in quantum information. The theoretical results are in good agreement

with the measured values [31]. The EPR peaks are obtained in terms of the high-order level splitting formula and eigenvectors from which the value of exchange coupling $J = 0.10$ K is determined and is seen in accord with the result of the resonance quantum tunneling [25–29]. Both experimental and theoretical investigations of EPR for the supermolecular dimers are of great importance for a better understanding the dynamics of such systems which are potential devices for quantum computing.

This work was supported by the Natural Science Foundation of China under Grant No. 10475053.

Appendix A: Eigenvectors

$$|\psi_1\rangle_S = \left| -\frac{9}{2}, -\frac{9}{2} \right\rangle,$$

$$\begin{aligned} |\psi_2\rangle_{S,A} &= \frac{1}{\sqrt{2}} \left| -\frac{9}{2}, -\frac{7}{2} \right\rangle_{S,A} \\ &= \frac{1}{\sqrt{2}} \left(\left| -\frac{9}{2}, -\frac{7}{2} \right\rangle \pm \left| -\frac{7}{2}, -\frac{9}{2} \right\rangle \right), \end{aligned}$$

$$|\psi_3\rangle_A = \frac{1}{\sqrt{2}} \left| -\frac{9}{2}, -\frac{5}{2} \right\rangle_A,$$

$$\begin{aligned}
|\psi_3\rangle_S &= 0.64013 \left| -\frac{9}{2}, -\frac{5}{2} \right\rangle_S - 0.42482 \left| -\frac{7}{2}, -\frac{7}{2} \right\rangle_S, & |\psi_{11}\rangle_S &= 0.6887 \left| -\frac{7}{2}, -\frac{1}{2} \right\rangle_S + 0.07793 \left| -\frac{9}{2}, \frac{1}{2} \right\rangle_S \\
&&&- 0.14008 \left| -\frac{5}{2}, -\frac{3}{2} \right\rangle_S, \\
|\psi_4\rangle_S &= 0.97356 \left| -\frac{7}{2}, -\frac{7}{2} \right\rangle_S + 0.16152 \left| -\frac{9}{2}, -\frac{5}{2} \right\rangle_S, & |\psi_{11}\rangle_A &= 0.65389 \left| -\frac{7}{2}, -\frac{1}{2} \right\rangle_A + 0.074 \left| -\frac{9}{2}, \frac{1}{2} \right\rangle_A \\
|\psi_5\rangle_S &= 0.69909 \left| -\frac{9}{2}, -\frac{3}{2} \right\rangle_S - 0.1062 \left| -\frac{7}{2}, -\frac{5}{2} \right\rangle_S, &&- 0.25876 \left| -\frac{5}{2}, -\frac{3}{2} \right\rangle_A, \\
|\psi_5\rangle_A &= 0.68721 \left| -\frac{9}{2}, -\frac{3}{2} \right\rangle_A - 0.16656 \left| -\frac{7}{2}, -\frac{5}{2} \right\rangle_A, & |\psi_{12}\rangle_{S,A} &= 0.67168 \left| -\frac{5}{2}, -\frac{3}{2} \right\rangle_{S,A} \\
|\psi_6\rangle_{S,A} &= 0.69375 \left| -\frac{7}{2}, -\frac{5}{2} \right\rangle_{S,A} + 0.13677 \left| -\frac{9}{2}, -\frac{3}{2} \right\rangle_{S,A}, &&+ 0.20121 \left| -\frac{7}{2}, -\frac{1}{2} \right\rangle_{S,A} + 0.09147 \left| -\frac{9}{2}, \frac{1}{2} \right\rangle_{S,A}, \\
|\psi_7\rangle_S &= 0.6992 \left| -\frac{9}{2}, -\frac{1}{2} \right\rangle_S - 0.10364 \left| -\frac{7}{2}, -\frac{3}{2} \right\rangle_S & |\psi_{13}\rangle_S &= 0.70425 \left| -\frac{9}{2}, \frac{3}{2} \right\rangle_S - 0.0633 \left| -\frac{7}{2}, \frac{1}{2} \right\rangle_S \\
&+ 0.02744 \left| -\frac{5}{2}, -\frac{5}{2} \right\rangle, &&+ 0.0049 \left| -\frac{5}{2}, -\frac{1}{2} \right\rangle_S - 7.49 \times 10^{-4} \left| -\frac{3}{2}, -\frac{3}{2} \right\rangle, \\
|\psi_7\rangle_A &= 0.70017 \left| -\frac{9}{2}, -\frac{1}{2} \right\rangle_A - 0.09882 \left| -\frac{7}{2}, -\frac{3}{2} \right\rangle_A, & |\psi_{13}\rangle_A &= 0.70425 \left| -\frac{9}{2}, \frac{3}{2} \right\rangle_A - 0.06328 \left| -\frac{7}{2}, \frac{1}{2} \right\rangle_A \\
&&&+ 0.00484 \left| -\frac{5}{2}, -\frac{1}{2} \right\rangle_A, \\
|\psi_8\rangle_S &= 0.55604 \left| -\frac{7}{2}, -\frac{3}{2} \right\rangle_S + 0.08045 \left| -\frac{9}{2}, -\frac{1}{2} \right\rangle_S & |\psi_{14}\rangle_S &= 0.68766 \left| -\frac{7}{2}, \frac{1}{2} \right\rangle_S + 0.0618 \left| -\frac{9}{2}, \frac{3}{2} \right\rangle_S \\
&- 0.6072 \left| -\frac{5}{2}, -\frac{5}{2} \right\rangle, &&- 0.14849 \left| -\frac{5}{2}, -\frac{1}{2} \right\rangle_S + 0.04995 \left| -\frac{3}{2}, -\frac{3}{2} \right\rangle, \\
|\psi_8\rangle_A &= 0.69982 \left| -\frac{7}{2}, -\frac{3}{2} \right\rangle_A + 0.10125 \left| -\frac{9}{2}, -\frac{1}{2} \right\rangle_A, & |\psi_{14}\rangle_A &= 0.69083 \left| -\frac{7}{2}, \frac{1}{2} \right\rangle_A + 0.06208 \left| -\frac{9}{2}, \frac{3}{2} \right\rangle_A \\
&&&- 0.13749 \left| -\frac{5}{2}, -\frac{1}{2} \right\rangle_A, \\
|\psi_9\rangle_S &= 0.93217 \left| -\frac{5}{2}, -\frac{5}{2} \right\rangle + 0.25448 \left| -\frac{7}{2}, -\frac{3}{2} \right\rangle_S & |\psi_{15}\rangle_S &= 0.49541 \left| -\frac{5}{2}, -\frac{1}{2} \right\rangle_S + 0.10279 \left| -\frac{7}{2}, \frac{1}{2} \right\rangle_S \\
&+ 0.02767 \left| -\frac{9}{2}, -\frac{1}{2} \right\rangle_S, &&+ 0.00581 \left| -\frac{9}{2}, \frac{3}{2} \right\rangle_S - 0.69853 \left| -\frac{3}{2}, -\frac{3}{2} \right\rangle, \\
|\psi_{10}\rangle_S &= 0.7026 \left| -\frac{9}{2}, \frac{1}{2} \right\rangle_S - 0.07938 \left| -\frac{7}{2}, -\frac{1}{2} \right\rangle_S & |\psi_{15}\rangle_A &= 0.69232 \left| -\frac{5}{2}, -\frac{1}{2} \right\rangle_A + 0.14364 \left| -\frac{7}{2}, \frac{1}{2} \right\rangle_A \\
&+ 0.00728 \left| -\frac{5}{2}, -\frac{3}{2} \right\rangle_S, &&+ 0.00812 \left| -\frac{9}{2}, \frac{3}{2} \right\rangle_A,
\end{aligned}$$

$$\begin{aligned}
|\psi_{16}\rangle_S &= 0.8928 \left| -\frac{3}{2}, -\frac{3}{2} \right\rangle + 0.31471 \left| -\frac{5}{2}, -\frac{1}{2} \right\rangle_S \\
&\quad + 0.04908 \left| -\frac{7}{2}, \frac{1}{2} \right\rangle_S + 0.00247 \left| -\frac{9}{2}, \frac{3}{2} \right\rangle_S, \\
|\psi_{17}\rangle_S &= 0.70536 \left| -\frac{9}{2}, \frac{5}{2} \right\rangle_S - 0.04963 \left| -\frac{7}{2}, \frac{3}{2} \right\rangle_S \\
&\quad + 3.012 \times 10^{-3} \left| -\frac{5}{2}, \frac{1}{2} \right\rangle_S - 1.68 \times 10^{-4} \left| -\frac{3}{2}, -\frac{1}{2} \right\rangle_S, \\
|\psi_{17}\rangle_A &= 0.70536 \left| -\frac{9}{2}, \frac{5}{2} \right\rangle_A - 0.04963 \left| -\frac{7}{2}, \frac{3}{2} \right\rangle_A \\
&\quad + 3.012 \times 10^{-3} \left| -\frac{5}{2}, \frac{1}{2} \right\rangle_A - 0.00019 \left| -\frac{3}{2}, -\frac{1}{2} \right\rangle_A, \\
|\psi_{18}\rangle_S &= 0.69716 \left| -\frac{7}{2}, \frac{3}{2} \right\rangle_S + 0.04905 \left| -\frac{9}{2}, \frac{5}{2} \right\rangle_S \\
&\quad - 0.10696 \left| -\frac{5}{2}, \frac{1}{2} \right\rangle_S + 0.01129 \left| -\frac{3}{2}, -\frac{1}{2} \right\rangle_S, \\
|\psi_{18}\rangle_A &= 0.69696 \left| -\frac{7}{2}, \frac{3}{2} \right\rangle_A + 0.04904 \left| -\frac{9}{2}, \frac{5}{2} \right\rangle_A \\
&\quad - 0.10782 \left| -\frac{5}{2}, \frac{1}{2} \right\rangle_A + 0.01455 \left| -\frac{3}{2}, -\frac{1}{2} \right\rangle_A, \\
|\psi_{19}\rangle_S &= 0.68215 \left| -\frac{5}{2}, \frac{1}{2} \right\rangle_S + 0.10494 \left| -\frac{7}{2}, \frac{3}{2} \right\rangle_S \\
&\quad + 0.00447 \left| -\frac{9}{2}, \frac{5}{2} \right\rangle_S - 0.15375 \left| -\frac{3}{2}, -\frac{1}{2} \right\rangle_S, \\
|\psi_{19}\rangle_A &= 0.62554 \left| -\frac{5}{2}, \frac{1}{2} \right\rangle_A + 0.09623 \left| -\frac{7}{2}, \frac{3}{2} \right\rangle_A \\
&\quad + 0.0041 \left| -\frac{9}{2}, \frac{5}{2} \right\rangle_A - 0.3153 \left| -\frac{3}{2}, -\frac{1}{2} \right\rangle_A, \\
|\psi_{20}\rangle_{S,A} &= 0.66389 \left| -\frac{3}{2}, -\frac{1}{2} \right\rangle_{S,A} + 0.24213 \left| -\frac{5}{2}, \frac{1}{2} \right\rangle_{S,A} \\
&\quad + 0.02495 \left| -\frac{7}{2}, \frac{3}{2} \right\rangle_{S,A} + 0.00089 \left| -\frac{9}{2}, \frac{5}{2} \right\rangle_{S,A}, \\
|\psi_{21}\rangle_S &= 0.70614 \left| -\frac{9}{2}, \frac{7}{2} \right\rangle_S - 0.03701 \left| -\frac{7}{2}, \frac{5}{2} \right\rangle_S \\
&\quad + 1.75 \times 10^{-3} \left| -\frac{5}{2}, \frac{3}{2} \right\rangle_S \\
&\quad - 8.163 \times 10^{-5} \left| -\frac{3}{2}, \frac{1}{2} \right\rangle_S + 7.77 \times 10^{-6} \left| -\frac{1}{2}, -\frac{1}{2} \right\rangle, \\
|\psi_{21}\rangle_A &= 0.70614 \left| -\frac{9}{2}, \frac{7}{2} \right\rangle_A - 0.03701 \left| -\frac{7}{2}, \frac{5}{2} \right\rangle_S \\
&\quad + 1.75 \times 10^{-3} \left| -\frac{5}{2}, \frac{3}{2} \right\rangle_A \\
&\quad - 8.163 \times 10^{-5} \left| -\frac{3}{2}, \frac{1}{2} \right\rangle_A, \\
|\psi_{22}\rangle_S &= 0.70148 \left| -\frac{7}{2}, \frac{5}{2} \right\rangle_S + 0.03676 \left| -\frac{9}{2}, \frac{7}{2} \right\rangle_S \\
&\quad - 0.08077 \left| -\frac{5}{2}, \frac{3}{2} \right\rangle_S \\
&\quad + 0.00723 \left| -\frac{3}{2}, \frac{1}{2} \right\rangle_S - 1.236 \times 10^{-3} \left| -\frac{1}{2}, -\frac{1}{2} \right\rangle, \\
|\psi_{22}\rangle_A &= 0.70148 \left| -\frac{7}{2}, \frac{5}{2} \right\rangle_S + 0.03676 \left| -\frac{9}{2}, \frac{7}{2} \right\rangle_A \\
&\quad - 0.08075 \left| -\frac{5}{2}, \frac{3}{2} \right\rangle_A + 0.0071 \left| -\frac{3}{2}, \frac{1}{2} \right\rangle_A, \\
|\psi_{23}\rangle_S &= 0.6801 \left| -\frac{5}{2}, \frac{3}{2} \right\rangle_S + 0.0783 \left| -\frac{7}{2}, \frac{5}{2} \right\rangle_S \\
&\quad + 0.00242 \left| -\frac{9}{2}, \frac{7}{2} \right\rangle_S - 0.17111 \left| -\frac{3}{2}, \frac{1}{2} \right\rangle_S \\
&\quad + 0.0639 \left| -\frac{1}{2}, -\frac{1}{2} \right\rangle, \\
|\psi_{23}\rangle_A &= 0.68525 \left| -\frac{5}{2}, \frac{3}{2} \right\rangle_A + 0.07889 \left| -\frac{7}{2}, \frac{5}{2} \right\rangle_S \\
&\quad + 0.00244 \left| -\frac{9}{2}, \frac{7}{2} \right\rangle_A - 0.15559 \left| -\frac{3}{2}, \frac{1}{2} \right\rangle_A, \\
|\psi_{24}\rangle_S &= 0.46545 \left| -\frac{3}{2}, \frac{1}{2} \right\rangle_S + 0.1114 \left| -\frac{5}{2}, \frac{3}{2} \right\rangle_S \\
&\quad + 0.00807 \left| -\frac{7}{2}, \frac{5}{2} \right\rangle_S \\
&\quad + 2.01 \times 10^{-4} \left| -\frac{9}{2}, \frac{7}{2} \right\rangle_S - 0.73604 \left| -\frac{1}{2}, -\frac{1}{2} \right\rangle, \\
|\psi_{24}\rangle_A &= 0.68759 \left| -\frac{3}{2}, \frac{1}{2} \right\rangle_A + 0.16456 \left| -\frac{5}{2}, \frac{3}{2} \right\rangle_A \\
&\quad + 0.01192 \left| -\frac{7}{2}, \frac{5}{2} \right\rangle_S + 2.968 \times 10^{-4} \left| -\frac{9}{2}, \frac{7}{2} \right\rangle_A, \\
|\psi_{25}\rangle_S &= 0.86948 \left| -\frac{1}{2}, -\frac{1}{2} \right\rangle + 0.34374 \left| -\frac{3}{2}, \frac{1}{2} \right\rangle_S \\
&\quad + 0.06184 \left| -\frac{5}{2}, \frac{3}{2} \right\rangle_S \\
&\quad + 0.00399 \left| -\frac{7}{2}, \frac{5}{2} \right\rangle_S + 8.347 \times 10^{-5} \left| -\frac{9}{2}, \frac{7}{2} \right\rangle_S,
\end{aligned}$$

$$\begin{aligned}
|\psi_{26}\rangle_S &= 0.7067 \left| -\frac{9}{2}, \frac{9}{2} \right\rangle_S - 0.02399 \left| -\frac{7}{2}, \frac{7}{2} \right\rangle_S \\
&\quad + 8.41 \times 10^{-4} \left| -\frac{5}{2}, \frac{5}{2} \right\rangle_S \\
&\quad - 3.02 \times 10^{-5} \left| -\frac{3}{2}, \frac{3}{2} \right\rangle_S + 9.43 \times 10^{-7} \left| -\frac{1}{2}, \frac{1}{2} \right\rangle_S, \\
|\psi_{26}\rangle_A &= 0.7067 \left| -\frac{9}{2}, \frac{9}{2} \right\rangle_A - 0.02399 \left| -\frac{7}{2}, \frac{7}{2} \right\rangle_A \\
&\quad + 8.41 \times 10^{-4} \left| -\frac{5}{2}, \frac{5}{2} \right\rangle_A \\
&\quad - 3.02 \times 10^{-5} \left| -\frac{3}{2}, \frac{3}{2} \right\rangle_A + 1.1 \times 10^{-6} \left| -\frac{1}{2}, \frac{1}{2} \right\rangle_A, \\
|\psi_{27}\rangle_S &= 0.70427 \left| -\frac{7}{2}, \frac{7}{2} \right\rangle_S + 0.02391 \left| -\frac{9}{2}, \frac{9}{2} \right\rangle_S \\
&\quad - 0.05845 \left| -\frac{5}{2}, \frac{5}{2} \right\rangle_S \\
&\quad + 0.00385 \left| -\frac{3}{2}, \frac{3}{2} \right\rangle_S - 2.272 \times 10^{-4} \left| -\frac{1}{2}, \frac{1}{2} \right\rangle_S, \\
|\psi_{27}\rangle_A &= 0.70427 \left| -\frac{7}{2}, \frac{7}{2} \right\rangle_A + 0.02391 \left| -\frac{9}{2}, \frac{9}{2} \right\rangle_A \\
&\quad - 0.05845 \left| -\frac{5}{2}, \frac{5}{2} \right\rangle_A \\
&\quad + 0.00385 \left| -\frac{3}{2}, \frac{3}{2} \right\rangle_A - 2.56 \times 10^{-4} \left| -\frac{1}{2}, \frac{1}{2} \right\rangle_A, \\
|\psi_{28}\rangle_S &= 0.69505 \left| -\frac{5}{2}, \frac{5}{2} \right\rangle_S + 0.05768 \left| -\frac{7}{2}, \frac{7}{2} \right\rangle_S \\
&\quad + 1.133 \times 10^{-3} \left| -\frac{9}{2}, \frac{9}{2} \right\rangle_S \\
&\quad - 0.11579 \left| -\frac{3}{2}, \frac{3}{2} \right\rangle_S + 0.01288 \left| -\frac{1}{2}, \frac{1}{2} \right\rangle_S, \\
|\psi_{28}\rangle_A &= 0.69485 \left| -\frac{5}{2}, \frac{5}{2} \right\rangle_A + 0.05767 \left| -\frac{7}{2}, \frac{7}{2} \right\rangle_A \\
&\quad + 0.00113 \left| -\frac{9}{2}, \frac{9}{2} \right\rangle_A \\
&\quad - 0.11651 \left| -\frac{3}{2}, \frac{3}{2} \right\rangle_A + 0.01684 \left| -\frac{1}{2}, \frac{1}{2} \right\rangle_A, \\
|\psi_{29}\rangle_S &= 0.67998 \left| -\frac{3}{2}, \frac{3}{2} \right\rangle_S + 0.11365 \left| -\frac{5}{2}, \frac{5}{2} \right\rangle_S \\
&\quad + 0.00571 \left| -\frac{7}{2}, \frac{7}{2} \right\rangle_S \\
&\quad + 8.81 \times 10^{-5} \left| -\frac{9}{2}, \frac{9}{2} \right\rangle_S - 0.15712 \left| -\frac{1}{2}, \frac{1}{2} \right\rangle_S, \\
|\psi_{29}\rangle_A &= 0.61463 \left| -\frac{3}{2}, \frac{3}{2} \right\rangle_A + 0.10272 \left| -\frac{5}{2}, \frac{5}{2} \right\rangle_A \\
&\quad + 0.00516 \left| -\frac{7}{2}, \frac{7}{2} \right\rangle_A \\
&\quad + 7.96 \times 10^{-5} \left| -\frac{9}{2}, \frac{9}{2} \right\rangle_A - 0.33414 \left| -\frac{1}{2}, \frac{1}{2} \right\rangle_A, \\
|\psi_{30}\rangle_{S,A} &= 0.65883 \left| -\frac{1}{2}, \frac{1}{2} \right\rangle_{S,A} + 0.2552 \left| -\frac{3}{2}, \frac{3}{2} \right\rangle_{S,A} \\
&\quad + 0.02857 \left| -\frac{5}{2}, \frac{5}{2} \right\rangle_{S,A} \\
&\quad + 1.202 \times 10^{-3} \left| -\frac{7}{2}, \frac{7}{2} \right\rangle_{S,A} + 1.67 \times 10^{-5} \left| -\frac{9}{2}, \frac{9}{2} \right\rangle_{S,A}, \\
|\psi_{31}\rangle_S &= 0.70614 \left| \frac{9}{2}, -\frac{7}{2} \right\rangle_S - 0.03701 \left| \frac{7}{2}, -\frac{5}{2} \right\rangle_S \\
&\quad + 1.75 \times 10^{-3} \left| \frac{5}{2}, -\frac{3}{2} \right\rangle_S \\
&\quad - 8.163 \times 10^{-5} \left| \frac{3}{2}, -\frac{1}{2} \right\rangle_S + 7.77 \times 10^{-6} \left| \frac{1}{2}, \frac{1}{2} \right\rangle, \\
|\psi_{31}\rangle_A &= 0.70614 \left| \frac{9}{2}, -\frac{7}{2} \right\rangle_A - 0.03701 \left| \frac{7}{2}, -\frac{5}{2} \right\rangle_S \\
&\quad + 1.75 \times 10^{-3} \left| \frac{5}{2}, -\frac{3}{2} \right\rangle_A \\
&\quad - 8.163 \times 10^{-5} \left| \frac{3}{2}, -\frac{1}{2} \right\rangle_A, \\
|\psi_{32}\rangle_S &= 0.70148 \left| \frac{7}{2}, -\frac{5}{2} \right\rangle_S + 0.03676 \left| \frac{9}{2}, -\frac{7}{2} \right\rangle_S \\
&\quad - 0.08077 \left| \frac{5}{2}, -\frac{3}{2} \right\rangle_S + 0.00723 \left| \frac{3}{2}, -\frac{1}{2} \right\rangle_S \\
&\quad - 1.236 \times 10^{-3} \left| \frac{1}{2}, \frac{1}{2} \right\rangle, \\
|\psi_{32}\rangle_A &= 0.70148 \left| \frac{7}{2}, -\frac{5}{2} \right\rangle_S + 0.03676 \left| \frac{9}{2}, -\frac{7}{2} \right\rangle_A \\
&\quad - 0.08075 \left| \frac{5}{2}, -\frac{3}{2} \right\rangle_A + 0.0071 \left| \frac{3}{2}, -\frac{1}{2} \right\rangle_A, \\
|\psi_{33}\rangle_S &= 0.70536 \left| \frac{9}{2}, -\frac{5}{2} \right\rangle_S - 0.04963 \left| \frac{7}{2}, -\frac{3}{2} \right\rangle_S \\
&\quad + 3.012 \times 10^{-3} \left| \frac{5}{2}, -\frac{1}{2} \right\rangle_S - 1.68 \times 10^{-4} \left| \frac{3}{2}, \frac{1}{2} \right\rangle_S,
\end{aligned}$$

$$\begin{aligned}
|\psi_{33}\rangle_A &= 0.70536 \left| \frac{9}{2}, -\frac{5}{2} \right\rangle_A - 0.04963 \left| \frac{7}{2}, -\frac{3}{2} \right\rangle_A \\
&\quad + 3.012 \times 10^{-3} \left| \frac{5}{2}, -\frac{1}{2} \right\rangle_A - 0.00019 \left| \frac{3}{2}, \frac{1}{2} \right\rangle_A, \\
|\psi_{34}\rangle_S &= 0.69716 \left| \frac{7}{2}, -\frac{3}{2} \right\rangle_S + 0.04905 \left| \frac{9}{2}, -\frac{5}{2} \right\rangle_S \\
&\quad - 0.10696 \left| \frac{5}{2}, -\frac{1}{2} \right\rangle_S + 0.01129 \left| \frac{3}{2}, \frac{1}{2} \right\rangle_S, \\
|\psi_{34}\rangle_A &= 0.69696 \left| \frac{7}{2}, -\frac{3}{2} \right\rangle_A + 0.04904 \left| \frac{9}{2}, -\frac{5}{2} \right\rangle_A \\
&\quad - 0.10782 \left| \frac{5}{2}, -\frac{1}{2} \right\rangle_A + 0.01455 \left| \frac{3}{2}, \frac{1}{2} \right\rangle_A, \\
|\psi_{35}\rangle_S &= 0.70425 \left| \frac{9}{2}, -\frac{3}{2} \right\rangle_S - 0.0633 \left| \frac{7}{2}, -\frac{1}{2} \right\rangle_S \\
&\quad + 0.0049 \left| \frac{5}{2}, \frac{1}{2} \right\rangle_S - 7.49 \times 10^{-4} \left| \frac{3}{2}, \frac{3}{2} \right\rangle_S, \\
|\psi_{35}\rangle_A &= 0.70425 \left| \frac{9}{2}, -\frac{3}{2} \right\rangle_A - 0.06328 \left| \frac{7}{2}, -\frac{1}{2} \right\rangle_A \\
&\quad + 0.00484 \left| \frac{5}{2}, \frac{1}{2} \right\rangle_A, \\
|\psi_{36}\rangle_S &= 0.7026 \left| \frac{9}{2}, -\frac{1}{2} \right\rangle_S - 0.07938 \left| \frac{7}{2}, \frac{1}{2} \right\rangle_S \\
&\quad + 0.00728 \left| \frac{5}{2}, \frac{3}{2} \right\rangle_S, \\
|\psi_{36}\rangle_A &= 0.70256 \left| \frac{9}{2}, -\frac{1}{2} \right\rangle_A - 0.07964 \left| \frac{7}{2}, \frac{1}{2} \right\rangle_A \\
&\quad + 0.00846 \left| \frac{5}{2}, \frac{3}{2} \right\rangle_A.
\end{aligned}$$

References

1. R. Sessoli, D. Gatteschi, A. Caneschi, M.A. Novak, Nature **365**, 141 (1993)
2. S.M.J. Aubin et al., J. Am. Chem. Soc. **118**, 7746 (1996)
3. C. Boskovic et al., J. Am. Chem. Soc. **124**, 3725 (2002)
4. J.R. Friedman, M.P. Sarachik, J. Tejada, R. Ziolo, Phys. Rev. Lett. **76**, 3830 (1996)
5. L. Thomas, F. Lioni, R. Ballou, D. Gatteschi, R. Sessoli, B. Barbara, Nature **383**, 145 (1996)
6. C. Sangregorio, T. Ohm, C. Paulsen, R. Sessoli, D. Gatteschi, Phys. Rev. Lett. **78**, 4645 (1997)
7. S. Hill et al., Phys. Rev. Lett. **80**, 2453 (1998)
8. L. Bokacheva, A.D. Kent, M.A. Walters, Phys. Rev. Lett. **85**, 4803 (2000)
9. W. Wernsdorfer, R. Sessoli, Science **284**, 133 (1999)
10. A. Garg, Europhys. Lett. **22**, 205 (1993)
11. A. Caneschi, D. Gatteschi, C. Sangregorio, R. Sessoli, L. Sorace, A. Cornia, M.A. Novak, C. Paulsen, W. Wernsdorfer, J. Magn. Magn. Mater. **200**, 182 (1999)
12. J.-Q. Liang, H.J.W. Müller-Kirsten, D.K. Park, F. Zimmerschied, Phys. Rev. Lett. **81**, 216 (1998)
13. S.P. Kou, J.-Q. Liang, Y.-B. Zhang, X.-B. Wang, F.-C. Pu, Phys. Rev. B **59**, 6309 (1999)
14. J.-Q. Liang, Y.-B. Zhang, H.J.W. Müller-Kirsten, J.G. Zhou, F. Zimmerschied, F.-C. Pu, Phys. Rev. B **57**, 529 (1998)
15. J.-Q. Liang, H.J.W. Müller-Kirsten, D.K. Park, F.-C. Pu, Phys. Rev. B **61**, 8856 (2000)
16. Nie Yi-Hang, Jin Yan-Hong, J.-Q. Liang, F.-C. Pu, Phys. Rev. B **64**, 134417 (2001)
17. B. Zhou, J.-Q. Liang, F.-C. Pu, Phys. Rev. B **64**, 132407 (2001)
18. M.N. Leuenberger, D. Loss, Nature **410**, 789 (2001)
19. S.C. Benjamin, S. Bose, Phys. Rev. Lett. **90**, 247901 (2003)
20. F. Meier, J. Levy, D. Loss, Phys. Rev. B **68**, 134417 (2003)
21. K. Park, M.A. Novotny, N.S. Dalal, S. Hill, P.A. Rikvold, Phys. Rev. B **65**, 014426 (2002)
22. S. Hill, S. Maccagnano, K. Park, R.M. Achey, J.M. North, N.S. Dalal, Phys. Rev. B **65**, 224410 (2002)
23. K. Park, M.A. Novotny, N.S. Dalal, S. Hill, P.A. Rikvold, Phys. Rev. B **66**, 144409 (2002)
24. D. Zipse, J.M. North, N.S. Dalal, S. Hill, R.S. Edwards, Phys. Rev. B **68**, 184408 (2003)
25. W. Wernsdorfer, N. Aliaga-Alcalde, D.N. Hendrickson, G. Christou, Nature **416**, 406 (2002)
26. W. Wernsdorfer, N. Aliaga-Alcalde, R. Tiron, D.N. Hendrickson, G. Christou, J. Magn. Magn. Mater. **272-276**, 1037 (2004)
27. R. Tiron, W. Wernsdorfer, D. Foguet-Albiol, N. Aliaga-Alcalde, G. Christou, Phys. Rev. Lett. **91**, 227203 (2003)
28. W. Wernsdorfer, S. Bhaduri, R. Tiron, D.N. Hendrickson, G. Christou, Phys. Rev. Lett. **89**, 197201 (2002)
29. Kim Gwang-Hee, Phys. Rev. B **67**, 024421 (2003)
30. Su Yuanchang, Tao Ruibao, Phys. Rev. B **68**, 024431 (2003)
31. S. Hill, R.S. Edwards, N. Aliaga-Alcalde, G. Christou, Science **302**, 1015 (2003)
32. D.A. Garanin, J. Phys. A: Math. Gen. **24**, L61 (1991)
33. C.H. Bennett, H.J. Bernstein, S. Popescu, B. Schumacher, Phys. Rev. A **53**, 2046 (1996)